Soil carbon storage along a 46-year revegetation chronosequence in a desert area of northern China

Yong-Le Chen[a,b], Zhi-Shan Zhang[a,*], Yang Zhao[a], Yi-Gang Hu[a], Ding-Hai Zhang[c]

[a] Shapotou Desert Research and Experimental Station, Northwest Institute of Eco-Environment and Resources, Chinese Academy of Sciences, Lanzhou 730000, People's Republic of China
[b] College of Life Sciences and Oceanography, Shenzhen University, Shenzhen 518060, People's Republic of China
[c] College of Natural Sciences, Gansu Agricultural University, Lanzhou 730070, People's Republic of China

ABSTRACT

Soil contains the majority of terrestrial carbon; however, most studies only focus on soil organic carbon (SOC) in the first meter or even shallower layers, and soil inorganic carbon (SIC) and root-derived carbon (RDC) are often overlooked. Here, we investigated the distribution of soil carbon at a depth of 0–3.0 m over a 46-year revegetation chronosequence on moving sand dunes and evaluated the potential influence of soil water content on soil carbon. The SOC density increased significantly along the 0–3.0 m profile, and showed a faster increasing rate in shallow layer (0–0.4 m) than that of the deep layers below 0.4 m. Although the SIC density did not increase significantly, it accounted for > 65% of the total soil carbon in shallow layer and at least 82% in deep layer. The live and dead RDC increased significantly over the chronosequence in both shallow and deep layers. The RDC accounted for a small amount of the total soil carbon at an average of 3.19%. The SOC was closely linked with live RDC in both the shallow and deep layers. The soil water content was only positively correlated with the SOC in the shallow layer. The SOC storage in the shallow layer required 57.4 years to reach the level at the natural vegetation site, whereas the storage in the deep layers required > 100 years. Our results indicated that soil carbon accumulation is a slow process in both shallow and deep layers after revegetation, and the most notable increase in soil carbon was accounted by SOC. We suggest that SOC, SIC and RDC should be considered when assessing the effects of revegetation on soil carbon in water-limited ecosystems.

1. Introduction

Soil represents an important and effective carbon reservoir in terrestrial ecosystems, and it is expected to have a more substantial sink capacity than the associated vegetation; thus, soil has a considerable ability to sequester carbon for the mitigation of elevated atmospheric CO_2 (Schlesinger, 1990; Batjes, 1996; Lal, 2004a, 2004b; Schmidt et al., 2011). Soil in water-limited ecosystems, which account for 47.2% of the global terrestrial surface, is estimated to contain approximately 241 Pg soil organic carbon (SOC) in the top one meter and an even larger soil inorganic carbon (SIC) pool (Eswaran et al., 2000). Therefore, the soil carbon storage in these ecosystems must be quantified and its potential response to environmental changes, e.g. vegetation and soil changes, should be determined.

Complete assessments of the SOC, SIC, and RDC pool are particularly lacking, especially in water-limited ecosystems. Due to the faster sequestration rate of SOC, most studies have focused on SOC, only a few studies have documented the distribution and dynamics of SIC (Diaz-

Hernandez et al., 2003; Hirmas et al., 2010; Chang et al., 2012). However, SIC is a main constituent of soil carbon in these ecosystems, and recent studies have suggested that SIC sequestration through both biological and non-biological processes may be underestimated (Wohlfahrt et al., 2008; Lal, 2009; Li et al., 2015). Root system is also a frequently neglected carbon reservoir. Actually, the cumulative contribution of RDC is comparatively larger and the residence time of root tissues in soil is longer than other plant tissues (Rasse et al., 2005; Pierret et al., 2016). Considering the high belowground production of root systems, which are normally large and deep in water-limited ecosystems (Chapin et al., 1993), RDC should not be overlooked when assessing soil carbon.

Most individual studies and large-scale investigations only focused on the first meter of soil (Batjes, 1996), or at even shallower depths, generally due to difficulties and costs associated with deeper sampling. However, many previous studies have detected larger amounts of soil carbon in deeper soil profiles in water-limited ecosystems (Harrison et al., 2011; Rumpel and Kogel-Knabner, 2011; Harper and Tibbett,

2013); thus, deeper sampling is necessary. Furthermore, carbon turnover in deep soils is commonly slow, implying deep organic carbon has a longer residence time (Pierret et al., 2016). In water-limited environments, soil water is a key factor that controls the soil carbon stock and dynamics via its effects on plant carbon allocation, microbial activities, and soil aggregate formation (Jobbágy and Jackson, 2000; Rey et al., 2005; Moyano et al., 2013). In general, increased soil water will stimulate plant production in both aboveground and belowground parts, thereby benefiting SOC accumulation. Thus, soil water is involved in contributing new carbon to the SOC pool, as well as retaining the available SOC (Norton et al., 2012; Zhou et al., 2012; Mi et al., 2014; Verburg et al., 2014). Soil water is also a necessary participant in the deposition, dissolution and leaching of SIC (Lal, 2009). Former studies have investigated the relationships between soil water and SOC (Wynn et al., 2006; Yang et al., 2008), but few studies have mentioned SIC and considered the different soil carbon components simultaneously in deep soil.

In this study, we took advantage of a 46-year-old revegetation chronosequence on sand dunes of the Tengger Desert to quantify the distribution and dynamics of different soil carbon components (SOC, SIC and RDC). Long-term studies conducted in this area have documented improvements in the topsoil conditions, such as increases in fine soil particles and soil nutrient availability (Duan et al., 2004; Li et al., 2007a), and enhanced biogeochemical processes in the topsoil (Wang et al., 2006). The revegetated soil system changes occurred along with a significant decrease in the soil water content in the deep layer over the 46-year succession (Li et al., 2014). However, the effects of decreased soil water content on the soil carbon storage via alterations to the revegetated soil system remained unclear. To enhance our knowledge-base on this topic, this study aimed to (1) investigate the temporal changes of carbon in soil along 0–3.0 m profile over a 46-year-old revegetation chronosequence; (2) analyze the relationships between SOC, SIC, RDC, and soil water content; (3) evaluate the revegetation success based on the rate of soil carbon sequestration. To achieve these issues, we collected soil samples from three revegetation sites (with ages of 20, 29, and 46 years) and compared the results with those from a moving sand dune and a naturally vegetated site.

2. Materials and methods

2.1. Study sites

The study was conducted along the southeastern fringe of the Tengger Desert in northwestern China. This area is characterized as a transitional zone from sandy desert to steppe. Because of the considerable groundwater depth (> 80 m), it is not available to vegetation; therefore, precipitation is the sole source of soil water in the study area (Li et al., 2004). Along the transitional zone, five study sites were set up from east to west (Fig. 1).

Shapotou (37°32′ N, 105°02′ E, at an elevation of 1300 m AMSL) is a typical temperate desert region. The annual mean temperature is 10 °C, and the mean January and July temperatures are −6.9 and 24.3 °C, respectively. The annual mean wind velocity is 2.9 m s^{-1}, and the annual mean precipitation is 186 mm, of which 80% falls between May and September. Large and dense reticulated barchans sand dune chains are typical of the landscape, and an aeolian sandy soil is the main soil type. Moving sand dunes are dominated by *Hedysarum scoparium* Fisch. & C. A. Mey. and *Agriophyllum squarrosum* (L.) Moq., which provide cover of < 1%. Since the 1950s, a 16 km long, 500 m wide rain-fed revegetation protective system was established along both sides of the Baotou-Lanzhou Railway in this region to stabilize the moving sand dunes and prevent desert encroachment. Xerophytic shrubs were planted following the establishment of the sand barrier. Subsequently, revegetation was further developed in 1964, 1981, and 1990. After long-term revegetation efforts, a diversified ecosystem composed of planted xerophytic shrubs (mainly *Artemisia ordosica* Krasch., *Caragana*
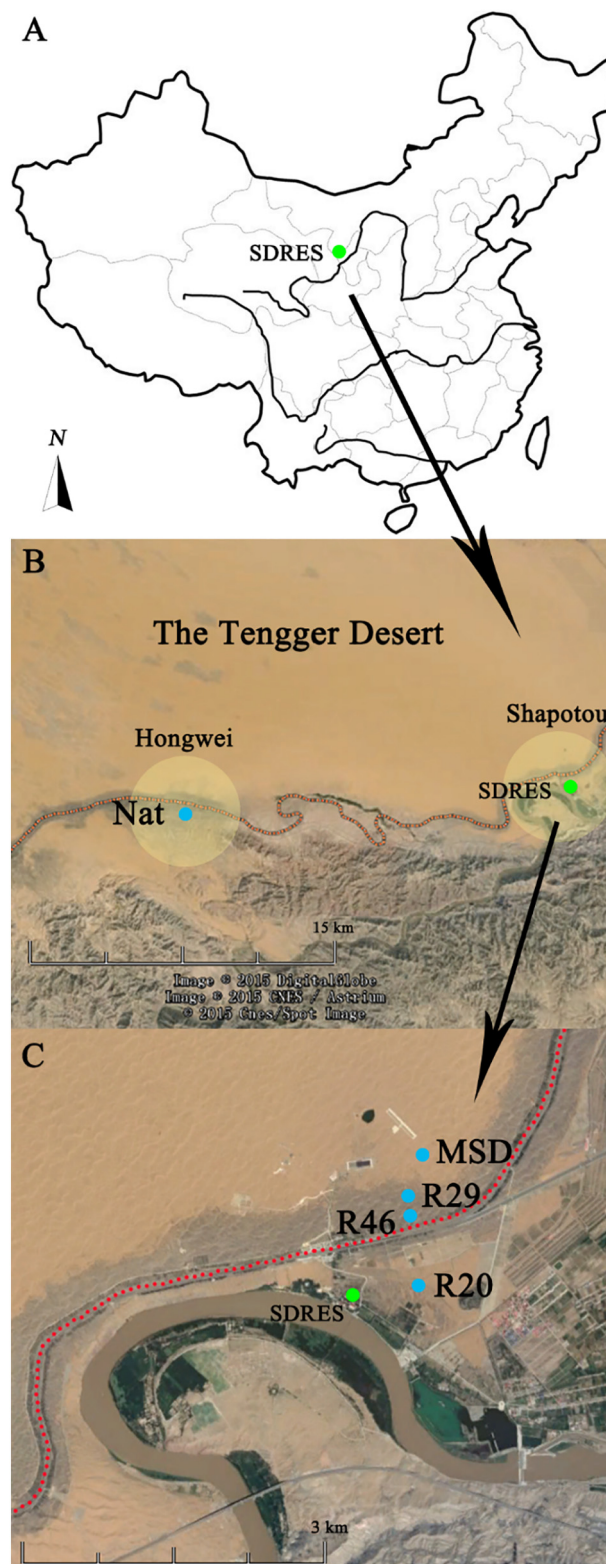
Fig. 1. Location of the five study sites (Nat, R46, R29, R20, and MSD site showed as blue points) in Hongwei and Shapotou region (showed by light yellow circles). SDRES (showed as green points) is Shapotou Desert Research and Experimental Station. Red dashed line is the Baotou-Lanzhou railway. A: Location of SDRES on the map of China. B: Location of Hongwei and Shapotou region along the Tengger Desert. C: Location of four sand dunes sites in Shapotou region. (For interpretation of the references to colour in this figure legend, the reader is referred to the web version of this article.)

korshinskii Kom., and *H. scoparium*), naturally occurring herbaceous species (*Eragrosti spoaeoides* P. Beauv., *Bassia dasyphylla* (Fisch. & et Mey.) O. Kuntze, *Corispermum patelliforme* Iljin, *Salsola ruthenica* Iljin, and *Aristida adscensionis* L.), and biological soil crusts (BSCs) evolved on sand-binding dunes. In this region, we chose three revegetation sites that were initially established in 1964, 1981, and 1990 (46, 29, and 20 years old, respectively), and the three sites are referred to as R46, R29, and R20, respectively. In addition, we also chose a control site on moving sand dunes (MSD) (Fig. 1).

Hongwei (37°27′ N, 104°46′ E, at an elevation of 1570 m AMSL) also lies in the vegetated protective system of the railway and it is characterized by undegraded native vegetation (referred as Nat) (Fig. 1) (Li et al., 2007b). Hongwei has the same climate, landscape and soil type as Shapotou, and the predominant plant species are shrubs, such as *A. ordosica*, *C. korshinskii*, *Ceratoides lateens* (J. F. Gmel.) Reveal et Holmgren, and *Oxytropis aciphylla* Ledeb., and herbaceous species, such as *Artemisia capillaries* Thunb., *Allium mongolicum* Regel, *S. ruthenica*, *Stipa breviflora* Griseb., *Cleistogenes songorica* (Roshev.) Ohwi, *Scorzonera divaricata* Turcz., and *Iris tenuifolia* Pall.

2.2. Sampling layout

Sampling was conducted in August 2010. At each site, ten 10 m × 10 m plots for the shrub survey were arranged along a line transect. The line transects at each site covered four typical geomorphologic types of sand dunes (all including dune crests, hollows between dunes, windward and leeward slopes), and the sample points were located on each topographic type at least twice. Here, four topographic types were served as four blocks and experiment design was modified as blocks within plot to avoid pseudo-replication. The means of soil carbon of each site were calculated from observations of four topographic types. In the present study, there were at least two plots in each topographic type. Three 1 m × 1 m quadrates for the herbs survey were set randomly within each shrub plot. In each shrub plot, one sample point for soil sampling was located near the center of the plot and one sample point for root sampling was located approximately 2 m away.

In each shrub plot, the height, density, and crown diameters (east to west and north to south) of each shrub were measured. The shrub cover in each quadrate was calculated as the sum of the cumulative canopy projected area of all shrubs assuming that crowns have an elliptical shape. The shrub biomass was estimated using a pre-built regression between the biomass of individual shrubs with the bulk canopy volume (from stem base to top of canopy). Specifically, we measured and mowed at least five individuals of dominant shrub species outside the revegetation protective system in Shapotou and Hongwei, and established numerical relations between shrub biomass and bulk canopy volume for each shrub species. In each herb quadrate, the density and cover were measured and then the aboveground components were mowed and weighed after 48 h of drying in an oven at 65 °C (Table 1).

2.3. Samples collection and laboratory analyses

A regular soil auger (AMS, Inc., USA) was used to collect soil samples at 0.1 m depth increments down to 1.0 m and then at 0.2 m depth increments down to 3.0 m. Each sample was divided into two subsamples, with one for soil carbon measurements and the other for soil water content measurements. For the soil carbon measurements, the soil samples collected from the same layer from two adjacent sample points were mixed into a composite. Five repetitions were performed at each site, and a total of 500 samples were obtained from all five sites. The soil samples were air dried and then passed through a 1 mm mesh to remove plant tissues and large sand particles. The SOC concentration was determined using the dichromate oxidation method (Bao and Shi, 2005). The SIC concentration was determined by a modified pressure calcimeter method (Sherrod et al., 2002). For the soil water content measurements, the samples were immediately transported to the laboratory and dried at 105 °C for 48 h, and then the gravimetric soil water content was measured. The results were then converted to the volumetric soil water content using the soil bulk density. For the soil bulk density measurement, the soil samples were collected by a specialized soil auger and a known weight cutting ring (0.05 m in depth and diameter), and they were weighed after drying at 105 °C for 48 h. After collecting soil samples from the five sites, ten neutron tubes were installed in the sampling points of each site. From January 2011, the volumetric soil water content was measured twice every month using a time domain reflectometry system (Field Scout TDR 300 Soil Moisture Meter, Spectrum Technologies, Inc.) in the upper 0.2 m layer and a neutron probe (CNC502DR, Beijing Nuclear, Inc.) in the 0.2–3.0 m layer (with 0.2 m increment). Rainfall was measured by standard tipping bucket rain gauge (Adolf Thies GMVH & Co·KG, Germany). The data from 2011 to 2013 are referenced in Fig. A1 and A2.

A homemade soil auger (0.1 m inner diameter and 0.2 m height) with a flat edge was used to collect soil samples that contained roots in 0.1 m increments down to 3.0 m. A total of 300 samples were collected at each site. Because of the dry and loose sandy soils, the watering method suggested by Zhang et al. (2009) was applied. The samples were transported to the laboratory and wet sieved through a 0.3 mm mesh to collect the live and dead roots and rhizosheath. Subsequently, the roots were dried at 65 °C for 48 h, and then weighed and grounded. The carbon concentration in the live and dead roots tissue was measured using a vario MACRO CUBE (Elementar Analysensysteme, Germany). The rhizosheath is produced by the expansion and contraction of the rhizosphere mucilage following diurnal wetting and drying of the root-soil interface, which pulls soil particles tightly together (McCully, 1999). In this study, rhizosheaths were washed, dried at 65 °C for 48 h, weighed and then grounded. Since the main component of rhizosheaths was calcium carbonate, the carbon concentration of calcium carbonate was considered to be equal to inorganic carbon concentration. Thus, the inorganic carbon concentration of the rhizosheath was determined by a modified pressure calcimeter method (Sherrod et al., 2002).

Table 1
Vegetation properties of the study sites (mean ± se). / denotes that no shrubs were found at the MSD site. The numerical relations between aboveground biomass (kg, y) and bulk canopy volume (m^{-3}, x) of three dominant shrubs in revegetation protective system: *C. korshinskii*, $y = 0.594x$; *A. ordosica*, $y = 0.143x$; *C. lateens*, $y = 0.317x$.

Site	Shrubs			Herbs			Total	
	Density (/100 m^{-2})	Cover (%)	Biomass (g m^{-2})	Density (/1 m^{-2})	Cover (%)	Biomass (g m^{-2})	Cover (%)	Biomass (g m^{-2})
MSD	/	/	/	4.39 ± 1.88	0.441 ± 0.202	0.174 ± 0.0947	0.441 ± 0.202	0.174 ± 0.0947
R20	24.0 ± 5.55	20.6 ± 4.62	67.5 ± 13.5	23.6 ± 8.20	6.83 ± 1.76	324 ± 64.8	27.4 ± 4.06	391 ± 58.2
R29	28.3 ± 4.69	17.0 ± 2.58	97.2 ± 13.3	17.2 ± 7.24	4.57 ± 1.30	544 ± 74.4	21.6 ± 2.29	641 ± 77.6
R46	26.5 ± 6.61	17.2 ± 3.98	74.5 ± 14.9	10.9 ± 3.78	4.01 ± 1.12	335 ± 67.1	21.1 ± 3.85	409 ± 75.7
Nat	37.4 ± 6.89	21.0 ± 5.77	125 ± 12.3	24.7 ± 5.33	6.77 ± 1.50	112 ± 11.0	27.5 ± 1.78	236 ± 20.8

2.4. Data analysis

For an individual layer, the SOC density (kg m^{-2}) and SIC density (kg m^{-2}) were calculated from the soil carbon concentration and soil bulk density:

$$SOC\ density = \sum_{i=1}^{n} SOC_i \times BD_i \times D_i/100$$

$$SIC\ density = \sum_{i=1}^{n} SIC_i \times BD_i \times D_i/100$$

where n is the number of horizons; SOC_i and SIC_i are soil organic and inorganic carbon concentrations (g kg^{-1}) for layer i, respectively; BD_i is soil bulk density (g cm^{-3}) for layer i; and D_i is the thickness (cm) of layer i. In the 0–0.4 m layer, D_i is 10 cm, and in the layer below 0.4 m, D_i is 20 cm.

In each layer, the RDC density (kg m^{-2}) of the live and dead roots and rhizosheath were calculated from the carbon concentration, respectively:

$$RDC\ density = \sum_{i=1}^{n} (M_i \times C_i/1000000)/S$$

where n is the number of horizons; M_i is the mass (g) of roots with different diameters or rhizosheaths for layer i; C_i is the organic carbon concentration (g kg^{-1}) of the roots with different diameters or inorganic carbon concentration (g kg^{-1}) of the rhizosheaths for layer i; and S is the cross-sectional area (m^{-2}) of the auger used for root sampling. The total RDC in each layer is the sum of the RDC for the roots and rhizosheaths.

Data on the soil carbon and RDC in the layers (0–0.4, 0.4–1.0, and 1.0–3.0 m) and the cumulative amounts (0–3.0 m), and corresponding ratios were compared among the five sites via a one-way ANOVA followed by Tukey's post hoc comparisons for significant differences. Regression analyses with linear, exponential, and logarithmic curves were used to quantify the relationships between RDC and soil carbon, and between soil water content and soil carbon and RDC. Because soil carbon accumulation is a long-term process, the averaged soil water contents monitored over three years (2011−2013) were used to perform regression analyses with SOC, SIC, and RDC. The linear, exponential, and logarithmic curves were also used to fit the relationships between the SOC density and revegetation age, and time required for the SOC in the revegetated soil to reach the level at the Nat site was estimated by the fitted model. Since degraded soil properties may not show a full recovery (Sparling et al., 2003), the time required to reach 90% of the value at the Nat site was also calculated. Statistical analyses were performed using SPSS 16.0 software (SPSS Inc., Chicago, USA), and graphs were created using Origin 8.0 software (Origin Lab, Northampton, USA).

3. Results

3.1. Distribution of soil carbon

In each site, the SOC concentration of 0–0.1 m layer was higher than that in the other layers, and the values increased gradually along the revegetation chronosequence but remained nearly constant below 0.4 m (Fig. A.3). The SIC concentration in 0–0.1 m of the R29, R46, and Nat sites was also higher than that of the other layers and increased along the revegetation chronosequence. For the soil layers below 0.1 m, it fluctuated between the minimum and maximum values. The higher SIC concentration of the MSD and R20 sites occurred in the 0.4–0.5 m layer.

Along the revegetation chronosequence, the SOC density increased significantly in the three layers (0–0.4, 0.4–1.0, and 1.0–3.0 m) and the whole profile (0–3.0 m) ($P < 0.001$) (Fig. 2). The value in the 0–3.0 m

profile of Nat site was 3.12 kg m^{-2} and significantly higher than that at MSD, R20, R29, and R46 sites (1.24, 1.25, 1.67, 1.71 kg m^{-2}, respectively). In 0–0.4 m layer, the SOC density at Nat site was significantly higher than that at MSD and R20 sites. The SOC ratios in the shallow layer (0–0.4 m) increased from 14.3% (MSD) to 30.4% (R46) ($P < 0.01$), whereas those in the deep layer (1.0–3.0 m) decreased from 64.8% (MSD) to 51.6% (R46) ($P < 0.001$) (Fig. 3, Table A.1 and A.2). There were no differences observed in SIC density and its ratios among the five sites (Fig. 2, Table A.1 and A.2). The SIC ratio of deep layer at each site was > 65%, where the ratio of shallow layer was < 14% (Fig. 3).

3.2. Distribution of root-derived carbon

The live and dead RDC density decreased as soil depth increased. Higher values were found in the 0–0.1 m, except for the live and dead RDC of MSD site in 2.4–2.5 and 2.5–2.6 m, respectively (Fig. A.4). The RDC density of rhizosheath at Nat site had the highest value in the 0–0.1 m layer and decreased along the vertical profile, while other sites were in deep layers.

The minimum value of total RDC in 0–3.0 m profile were 0.0114 kg m^{-2} at MSD site, and the maximum values was 0.299 kg m^{-2} at R46 sites (Fig. 2). The live and dead RDC density in three different layers of the 0–3.0 m profile increased significantly along the revegetation chronosequence (from MSD to R46 and Nat sites) (Fig. A.5). The ratios of live and RDC in 0–0.4 m layer increased significantly from MSD to R46 sites (from 21.6% to 64.7% and 12.6% to 64.0%, respectively), whereas ratios of dead roots in 1.0–3.0 m layer decreased significantly from 80.0% (MSD) to 18.6% (Nat) (Fig. 4). The ratios of the rhizosheath RDC in the deep layer of each site were > 50%.

3.3. Distribution of total carbon in soil

The density of soil total carbon (TC), including SOC, SIC, and RDC, only increased significantly along the revegetation chronosequence in 0–0.4 m layer ($P < 0.05$) (Fig. 2). In 0–0.4 m layer, the ratio of SOC accounted in TC increased significantly from the MSD (9.10%) to Nat sites (30.0%), whereas the ratio of SIC decreased from 90.9% to 60.8% along the revegetation chronosequence (Fig. 5). The ratio of RDC accounted little in TC, with average of 3.19%, and the highest value was observed at Nat site (6.52%). Throughout the entire 0–3.0 m profile, SOC at the Nat site accounted for 19.3% of TC, and this value was significantly higher than other sites. The SIC density of Nat site was lower than other sites, which presented values at > 87.0%.

### 3.4. Relationships of soil carbon, root-derived carbon and soil water content

Compared with the SIC, the RDC was more strongly related to the SOC (Table A.3). Additionally, fine root derived carbon had more positive relationships than dead root with SOC in both 0–0.4 m layer and 0–3.0 m profile ($P < 0.001$) (Fig. 6). SOC density was only significantly related to the soil water content in 0–0.4 m layer, which was fitted by exponential curve (R^2 = 0.657, $P < 0.001$) (Fig. 7). Significantly positive but weak correlations were found between live RDC and soil water content in shallow layers, while between dead and rhizosheath RDC with soil water content in deep layers (Table A.4).

3.5. Estimation of the rate of soil organic carbon sequestration

The relationships between SOC and revegetated age were successfully fitted by exponential curves, especially those of the 0–0.4 m and 0–3.0 m layers ($P < 0.01$) (Table 2). According to the estimation, the SOC of the 0–0.4 m layer required 57.4 and 53.0 years to reach the full and 90% level at the Nat site, respectively. As the depth increased, the recovery time also increased to at least 100 years. For example, the SOC in the 1.0–3.0 m of the revegetated sites required 176 years to reach the
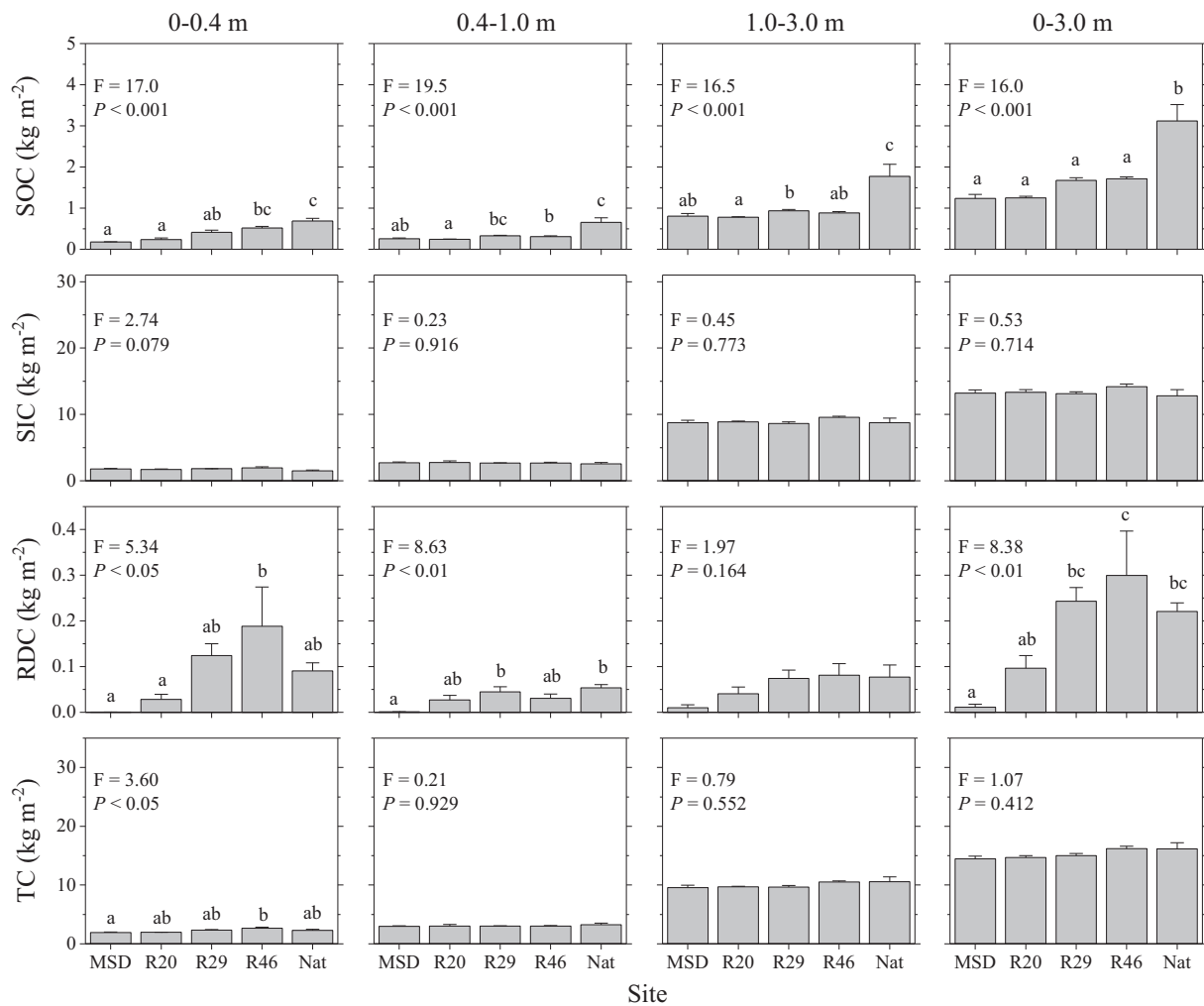
Fig. 2. Comparisons of soil carbon in different soil layers between the five sites. SOC, SIC, RDC, and TC represent soil organic carbon, soil inorganic carbon, root derived carbon, and total carbon in soils. All values were mean ± se (the same as below). Values with different letters are significant at $P < 0.05$.
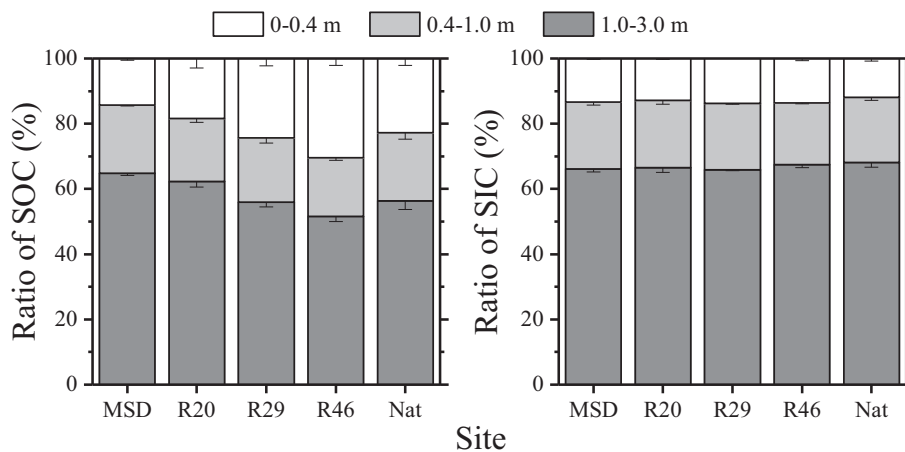
Fig. 3. Ratios of SOC and SIC in different soil layers accounted in the whole soil profile (0–3.0 m) at the five sites.

levels at the Nat site. In terms of the entire 0–3.0 m profile, the recovery time shortened but was still longer than that of the 0–0.4 m layer (Table 2).

4. Discussion

4.1. Effects of revegetation on soil carbon accumulation

Revegetation performed on moving sand dunes in different years formed a valuable succession chronosequence for evaluating the potential effects of revegetation on soil carbon accumulation in water-
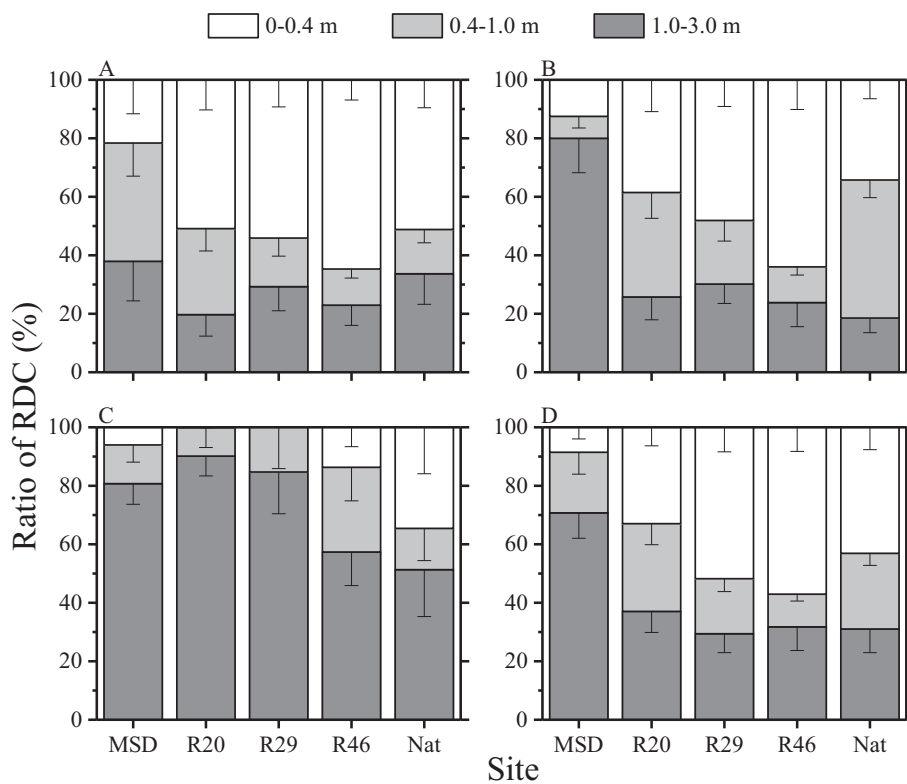
Fig. 4. Ratios of RDC in different soil layers accounted in the whole soil profile (0–3.0 m) at the five sites. A, B, C, and D shows live RDC, dead RDC, RDC in rhizosheath, and the total RDC.
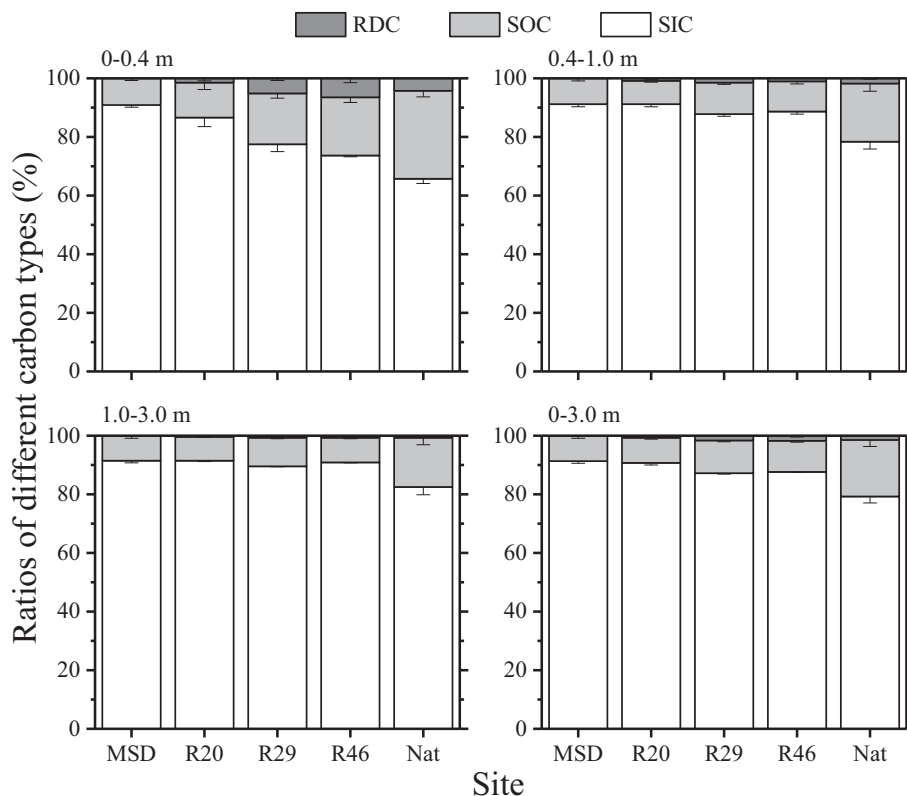

Fig. 5. Ratios of RDC, SOC, and SIC in total soil carbon within each soil layer.
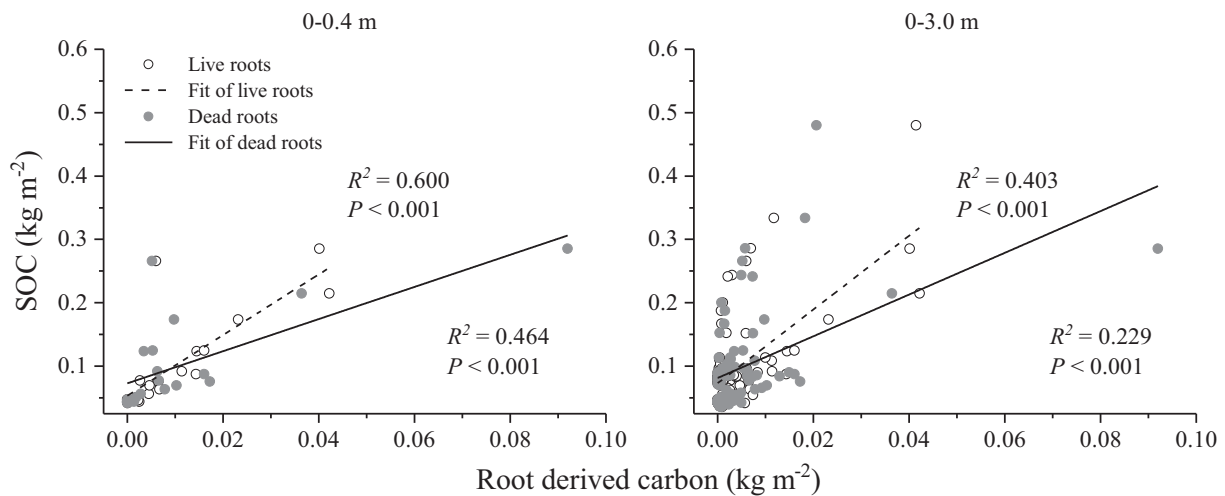
Fig. 6. Regression analyses between root derived carbon and SOC density in 0–0.4 and 0–3.0 m layers.
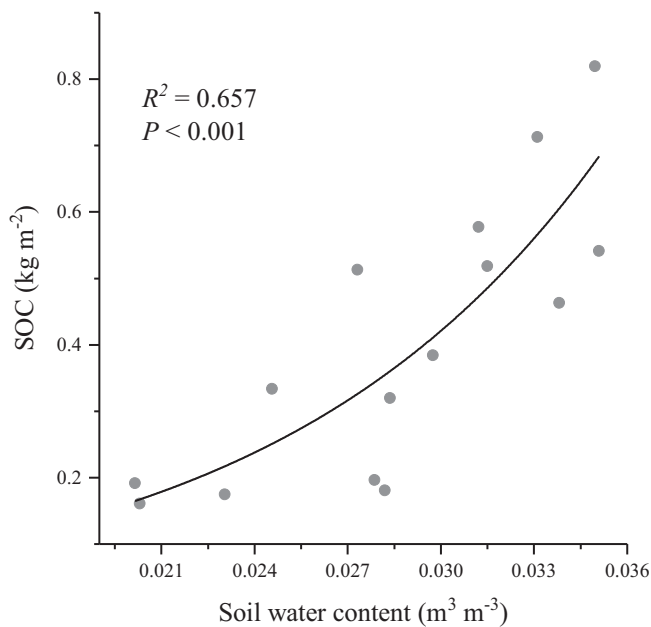

Fig. 7. Regression analyses between soil water content and SOC density in 0–0.4 m layer.

limited ecosystems. The results showed that only total carbon density of the shallow layers (0–0.4 m) increased significantly over the revegetation chronosequence (Fig. 2). In addition, the SOC ratio increased in the shallow layers but decreased in the deep layers, whereas the SIC ratio remained stable over the chronosequence (Fig. 3).

Prior land use was considered a primarily determinant of soil carbon accumulation following revegetation (Paul et al., 2002). In the present study, revegetation was conducted on sandy soils with poor productivity and commonly lack SOC. Thus, the soils may represent a

potential reserve for the rapid accumulation of SOC. Similar conclusions have drawn by many previous studies (Huang et al., 2012; Garcia-Franco et al., 2014), particularly in water-limited ecosystems (Berthrong et al., 2012). According to our results, the most significant changes were contributed by SOC. On the one hand, such increase should be related to the improved microenvironments induced by revegetation. The planted shrubs, naturally inhabited herbaceous species, the colonization and development of BSCs both produce additional organic matters, which increasing carbon input prior to the shallow soils (Li, 2012). Also, the increased clay content and strengthened biogeochemical cycles, such as nitrogen cycle will facilitate SOC accumulation (Jobbágy and Jackson, 2000; van Groenigen et al., 2006). On the other hand, the continuous accumulation of SOC may have been favored by the lower decomposition of SOC in dry environments (Grunzweig et al., 2007). Although rapid accumulation of SOC was observed, the full rehabilitation of SOC still required long time. The results showed that 57.4 years are required to reach the SOC level in the 0–0.4 m layer of Nat site. Li et al. (2007a) indicated the time for SOC in the 0–0.05 m layer to reach the 90% level of Nat site was 44-years. In the 0.4–1.0 m and 1.0–3.0 m layers, > 100 years were required. These results implicated that SOC accumulation rate is not only slow in shallow layers, but also in deep layers.

In this study, SIC showed a negligible increase, although its ratios showed a clear decreasing contribution to the total carbon over the revegetation chronosequence. The SIC pool accounted for at least 79.2% of the total carbon in the 0–3.0 m profile, which was similar to the value of 84.0% in arid and semi-arid areas of China (Mi et al., 2008). Generally, SIC maintains a relatively high concentration but a low rate of formation and dissolution (Lal, 2009). A study from the Loess Plateau reported that revegetation does not facilitate net SIC accumulation but leads to the redistribution of SIC along the soil profile (Chang et al., 2012). In our study, the slower accumulation of SIC than SOC was responsible for the declines in the SIC ratio. In dry soils, decreases in the soil water content or partial pressure of CO_2 or increases in the Ca^{2+} or HCO^{-3} concentration can lead to a favorable soil

Table 2
Relationships between SOC density in different soil layers and the age of revegetated dunes, and estimation of years needed to reach the full or 90% of SOC level (asymptote) at the Nat site.

Soil layer	Relationship	R^2	P	Asymptote (kg m^{-2})	Years to reach asymptote	90% of asymptote (kg m^{-2})	Years to reach 90% of asymptote
0–0.4 m	y = 0.175 ∗ exp. (0.0238x)	0.967	< 0.01	0.687	57.4	0.618	53.0
0.4–1.0 m	y = 0.234 ∗ exp. (0.00631x)	0.063	< 0.05	0.655	163	0.590	146
1.0–3.0 m	y = 0.710 ∗ exp. (0.00522x)	0.231	< 0.01	1.77	176	1.60	155
0–3.0 m	y = 1.10 ∗ exp. (0.00959x)	0.732	< 0.01	3.12	109	2.80	97.6

environment for SIC change (Wilding et al., 1990; Mi et al., 2008). The SIC distribution along a soil profile is also closely related to the infiltration of rainfall (Schlesinger and Pilmanis, 1998). Generally, the infiltration depth of rainwater depends on the rainfall characteristics (amount, intensity, duration, and inter-event time) (Wang et al., 2008) and soil surface conditions (such as BSCs) (Li, 2012). In this study, the low and variable rainfall regime together with the well-developed BSCs and topsoils with high water-holding capacity, resulted in a lack of rainwater infiltration at soil depths below 0.4 m following long-term revegetation (Wang et al., 2008; Li et al., 2010). These conditions further restrain the formation, leaching, and precipitation of carbonates.

4.2. Contribution of root-derived carbon to soil carbon

The RDC content and its ratios in total soil carbon were much lower than that of the soil carbon, and the average ratio of RDC to TC was 3.19% in the 0–0.4 m layer. However, RDC should not be overlooked because root systems provide the primary input of organic carbon into soil (Balesdent and Balabane, 1996; Rasse et al., 2005). As revealed by Zhang et al. (2008, 2009), root systems of dominant plants in present study area have a high turnover rate and will provide continuous contribution to the soil carbon pool. Our results showed that both the total RDC and its ratio to the total carbon increased over the chronosequence (Figs. 2 and 5). Available studies showed that most of the accumulated soil carbon is derived from root turnover, and deep-rooted species have considerable potential to sequester carbon in deep soil layers (Fisher et al., 1994; Hu et al., 2016). In our study, the shrubs selected for initial revegetation, such as *C. korshinskii* and *H. scoparium*, are deeply rooted; whereas the dwarf shrub *A. ordosica*, which is a key species in the latter successional phase, always distributes its roots within shallow soil layers (Zhang et al., 2008, 2009). Shallow-distributed root systems and increased plant biomass allocated to shallow layers may leave distinct imprints on the relative distribution of soil carbon along with depth (Fig. 6).

4.3. Influence of soil water content on carbon in soil

Our results showed that soil water content was only positively correlated with SOC of 0–0.4 m layer. This result was similar to the previous studies performed by Wynn et al. (2006) and Yang et al. (2008). In another study, Jobbágy and Jackson (2000) considered soil water content as a controlling factor of SOC. In present study site, fine particles in the shallow soil layer were shown to increase significantly over the revegetation chronosequence (Li et al., 2007a), which led to higher soil water availability. The positive response of the SOC may also be related to changes in the sand-binding revegetation which is driven by soil water (Li et al., 2014). After nearly 50 years of revegetation, the originally planted shrubs had been replaced by a multi-synusium composed of a few shrubs, a large number of herbaceous species and BSCs. These changes in the vegetation composition reflect variations in the soil water content and further contribute to the soil carbon (Jobbágy and Jackson, 2000; Yang et al., 2008). Differing from the sensitive response of fine root density to soil water content, only weak relationships were observed between soil water content and RDC. The main reason for this finding may be that the increased soil water content only stimulated root proliferation (Wynn et al., 2006) and do promote a higher root turnover rate (Pregitzer et al., 1993); in this manner, carbon was immediately input into soil and stored in roots. For deep layers, decreased deep-rooted shrubs and increased shallow-rooted herbaceous species in the revegetation areas led to a shallower distribution of the root systems. Thus, deep RDC does not correspond to soil water due to up-shifted of root systems and the lower decomposition rate of root residuals in deep soils (Harrison et al., 2011).

5. Conclusions

We investigated the changes in soil carbon storage along the 0–3.0 m soil profile, including SOC, SIC, and RDC following revegetation with xerophytic shrubs in a desert area of China. Over the 46-year revegetation chronosequence, SOC and total carbon in soils of the entire 0–3.0 m profile increased significantly. Our findings highlighted that improvement of soil carbon was a slow process, especially in deep soils, and predominant changes came from accumulation of SOC. SIC pool was larger than SOC pool, which accounts > 65% of the total carbon of soil in the shallow and 82% in the deep layers. In terms of the storage time, SIC pool was more durable. Though accounting a small proportion in the total carbon of soil, RDC closely linked with SOC, especially in the shallow layer. We demonstrated that the relative superior condition of soil water content in shallow layer lead to the accumulation of soil carbon. Further studies are needed to analyze the dynamic contribution of root-derived carbon to soil carbon, influences of soil properties on soil carbon with innovative approaches in such water-limited ecosystems.

Appendix A. Supplementary data

Supplementary data to this article can be found online at https://doi.org/10.1016/j.geoderma.2018.03.024.

References

Balesdent, J., Balabane, M., 1996. Major contribution of roots to soil carbon storage inferred from maize cultivated soils. Soil Biol. Biochem. 28, 1261–1263.

Bao, S., Shi, R. (Eds.), 2005. The Analysis of Soil Agriculturalization. China Agriculture Press, Beijing (in Chinese).

Batjes, N.H., 1996. Total carbon and nitrogen in the soils of the world. Eur. J. Soil Sci. 47, 151–163.

Berthrong, S.T., PIneiro, G., Jobbágy, E.G., Jackson, R.B., 2012. Soil C and N changes with afforestation of grasslands across gradients of precipitation and plantation age. Ecol. Appl. 22, 76–86.

Chang, R.Y., Fu, B.J., Liu, G.H., Wang, S., Yao, X.L., 2012. The effects of afforestation on soil organic and inorganic carbon: A case study of the Loess Plateau of China. Catena 95, 145–152.

Chapin, F.S., Autumn, K., Pugnaire, F., 1993. Evolution of suites of traits in response to environmental stress. Am. Nat. 142, S78–S92.

Diaz-Hernandez, J.L., Fernandez, E.B., Gonzalez, J.L., 2003. Organic and inorganic carbon in soils of semiarid regions: a case study from the Guadix-Baza basin (Southeast Spain). Geoderma 114, 65–80.

Duan, Z.H., Xiao, H.L., Li, X.R., Dong, Z.B., Gang, W., 2004. Evolution of soil properties on stabilized sands in the Tengger Desert, China. Geomorphology 59, 237–246.

Eswaran, H., Reich, P., Kimble, J., Beinroth, F., Padmanabhan, E., Moncharoen, P., 2000. Global carbon stocks. In: Lal, R., Kimble, J.M., Stewart, B.A., Eswaran, H. (Eds.), Global Climate Change and Pedogenic Carbonates. Lewis Publishers, Boca Raton.

Fisher, M.J., Rao, I.M., Ayarza, M.A., Lascano, C.E., Sanz, J.I., Thomas, R.J., Vera, R.R., 1994. Carbon storage by introduced deep-rooted grasses in the south-American savannas. Nature 371, 236–238.

Garcia-Franco, N., Wiesmeier, M., Goberna, M., Martínez-Mena, M., Albaladejo, J., 2014. Carbon dynamics after afforestation of semiarid shrublands: Implications of site preparation techniques. For. Ecol. Manag. 319, 107–115.

van Groenigen, K.J., Six, J., Hungate, B.A., de Graaff, M.A., van Breemen, N., van Kessel, C., 2006. Element interactions limit soil carbon storage. Proc. Natl. Acad. Sci. 103, 6571–6574.

Grunzweig, J.M., Gelfand, I., Fried, Y., Yakir, D., 2007. Biogeochemical factors contributing to enhanced carbon storage following afforestation of a semi-arid shrubland. Biogeosciences 4, 891–904.

Harper, R.J., Tibbett, M., 2013. The hidden organic carbon in deep mineral soils. Plant Soil 368, 641–648.

Harrison, R.B., Footen, P.W., Strahm, B.D., 2011. Deep soil horizons: contribution and importance to soil carbon pools and in assessing whole-ecosystem response to management and global change. For. Sci. 57, 67–76.

Hirmas, D.R., Amrhein, C., Graham, R.C., 2010. Spatial and process-based modeling of soil inorganic carbon storage in an arid piedmont. Geoderma 154, 486–494.

Hu, Y.L., Zeng, D.H., Ma, X.Q., Chang, S.X., 2016. Root rather than leaf litter input drives soil carbon sequestration after afforestation on a marginal cropland. For. Ecol. Manag. 362, 38–45.

Huang, G., Zhao, X.Y., Li, Y.Q., Cui, J.Y., 2012. Restoration of shrub communities elevates organic carbon in arid soils of northwestern China. Soil Biol. Biochem. 47, 123–132.

Jobbágy, E.G., Jackson, R.B., 2000. The vertical distribution of soil organic carbon and its relation to climate and vegetation. Ecol. Appl. 10, 423–436.

Lal, R., 2004a. Soil carbon sequestration impacts on global climate change and food security. Science 304, 1623–1627.

Lal, R., 2004b. Soil carbon sequestration to mitigate climate change. Geoderma 123, 1–22.

Lal, R., 2009. Sequestering carbon in soils of arid ecosystems. Land Degrad. Dev. 20, 441–454.

Li, X.R. (Ed.), 2012. Eco-Hydrology of Biological Soil Crusts in Desert Regions of China. Higher Education Press, Beijing (in Chinese).

Li, X.R., Ma, F.Y., Xiao, H.L., Wang, X.P., Kim, K.C., 2004. Long-term effects of re-vegetation on soil water content of sand dunes in arid region of northern China. J. Arid Environ. 57, 1–16.

Li, X.R., He, M.Z., Duan, Z.H., Xiao, H.L., Jia, X.H., 2007a. Recovery of topsoil physico-chemical properties in revegetated sites in the sand-burial ecosystems of the Tengger Desert, northern China. Geomorphology 88, 254–256.

Li, X.R., Kong, D.S., Tan, H.J., Wang, X.P., 2007b. Changes in soil and vegetation fol-lowing stabilisation of dunes in the southeastern fringe of the Tengger Desert, China. Plant Soil 300, 221–231.

Li, X.R., Tian, F., Jia, R.L., Zhang, Z.S., Liu, L.C., 2010. Do biological soil crusts determine vegetation changes in sandy deserts? Implications for managing artificial vegetation. Hydrol. Process. 24, 3621–3630.

Li, X.R., Zhang, Z.S., Tan, H.J., Gao, Y.H., Liu, L.C., Wang, X.P., 2014. Ecological re-storation and recovery in the wind-blown sand hazard areas of northern China: re-lationship between soil water and carrying capacity for vegetation in the Tengger Desert. Sci. China Life Sci. 57, 539–548.

Li, Y., Wang, Y.G., Houghton, R.A., Tang, L.S., 2015. Hidden carbon sink beneath desert. Geophys. Res. Lett. 42, 5880–5887.

McCully, M.E., 1999. Roots in soil: unearthing the complexities of roots and their rhi-zospheres. Annu. Rev. Plant Biol. 50, 695–718.

Mi, N., Wang, S.Q., Liu, J.Y., Yu, G.R., Zhang, W.J., Jobbaagy, E., 2008. Soil inorganic carbon storage pattern in China. Glob. Chang. Biol. 14, 2380–2387.

Mi, J., Li, J.J., Chen, D.M., Xie, Y.C., Bai, Y.F., 2014. Predominant control of moisture on soil organic carbon mineralization across a broad range of arid and semiarid eco-systems on the Mongolia plateau. Landsc. Ecol. 30, 1683–1699.

Moyano, F.E., Manzoni, S., Chenu, C., 2013. Responses of soil heterotrophic respiration to moisture availability: an exploration of processes and models. Soil Biol. Biochem. 59, 72–85.

Norton, U., Saetre, P., Hooker, T.D., Stark, J.M., 2012. Vegetation and moisture controls on soil carbon mineralization in semiarid environments. Soil Sci. Soc. Am. J. 76, 1038–1047.

Paul, K.I., Polglase, P.J., Nyakuengama, J.G., Khanna, P.K., 2002. Change in soil carbon following afforestation. For. Ecol. Manag. 168, 241–257.

Pierret, A., Maeght, J.-L., Clément, C., Montoroi, J.-P., Hartmann, C., Gonkhamdee, S., 2016. Understanding deep roots and their functions in ecosystems: an advocacy for more unconventional research. Ann. Bot. 2016, 1–15.

Pregitzer, K.S., Hendrick, R.L., Fogel, R., 1993. The demography of fine roots in response to patches of water and nitrogen. New Phytol. 125, 575–580.

Rasse, D.P., Rumpel, C., Dignac, M.F., 2005. Is soil carbon mostly root carbon? Mechanisms for a specific stabilisation. Plant Soil 269, 341–356.

Rey, A., Petsikos, C., Jarvis, P.G., Grace, J., 2005. Effect of temperature and moisture on rates of carbon mineralization in a Mediterranean oak forest soil under controlled and field conditions. Eur. J. Soil Sci. 56, 589–599.

Rumpel, C., Kogel-Knabner, I., 2011. Deep soil organic matter-a key but poorly under-stood component of terrestrial C cycle. Plant Soil 338, 143–158.

Schlesinger, W.H., 1990. Evidence from chronosequence studies for a low carbon-storage potential of soils. Nature 348, 232–234.

Schlesinger, W.H., Pilmanis, A.M., 1998. Plant-soil interactions in deserts. Biogeochemistry 42, 169–187.

Schmidt, M.W.I., Torn, M.S., Abiven, S., Dittmar, T., Guggenberger, G., Janssens, I.A., Kleber, M., Kogel-Knabner, I., Lehmann, J., Manning, D.A.C., Nannipieri, P., Rasse, D.P., Weiner, S., Trumbore, S.E., 2011. Persistence of soil organic matter as an eco-system property. Nature 478, 49–56.

Sherrod, L., Dunn, G., Peterson, G., Kolberg, R., 2002. Inorganic carbon analysis by modified pressure-calcimeter method. Soil Sci. Soc. Am. J. 66, 299–305.

Sparling, G., Ross, D., Trustrum, N., Arnold, G., West, A., Speir, T., Schipper, L., 2003. Recovery topsoil characteristics after landslip erosion in dry hill country of New Zealand, and a test of the spacefor-time hypothesis. Soil Biol. Biochem. 35, 1575–1586.

Verburg, P.S.J., Kapitzke, S.E., Stevenson, B.A., Bisiaux, M., 2014. Carbon allocation in *Larrea tridentata* plant-soil systems as affected by elevated soil moisture and N availability. Plant Soil 378, 227–238.

Wang, X.P., Li, X.R., Xiao, H.L., Pan, Y.X., 2006. Evolutionary characteristics of the ar-tificially revegetated shrub ecosystem in the Tengger Desert, northern China. Ecol. Res. 21, 415–424.

Wang, X.P., Cui, Y., Pan, Y.X., Li, X.R., Yu, Z., Young, M.H., 2008. Effects of rainfall characteristics on infiltration and redistribution patterns in revegetation-stabilized desert ecosystems. J. Hydrol. 358, 134–143.

Wilding, L.P., West, L.T., Drees, L.R., 1990. Field and laboratory identification of calcic and petrocalcic horizons. In: Kimble, J.M., Nettleton, W.D. (Eds.), Proceedings of the Fourth International Soil Correlation Meeting (ISCOM IV) Characterization, Classification, and Utilization of Aridisols. Part A: Papers. US Department of Agriculture-Soil Conservation Service, Lincoln.

Wohlfahrt, G., Fenstermaker, L.F., Arnone, J.A., 2008. Large annual net ecosystem CO_2 uptake of a Mojave Desert ecosystem. Glob. Chang. Biol. 14, 1475–1487.

Wynn, J.G., Bird, M.I., Vellen, L., Grand-Clement, E., Carter, J., Berry, S.L., 2006. Continental-scale measurement of the soil organic carbon pool with climatic, edaphic, and biotic controls. Glob. Biogeochem. Cycles 20.

Yang, Y.H., Fang, J.Y., Tang, Y.H., Ji, C.J., Zheng, C.Y., He, J.S., Zhu, B.A., 2008. Storage, patterns and controls of soil organic carbon in the Tibetan grasslands. Glob. Chang. Biol. 14, 1592–1599.

Zhang, Z.S., Li, X.R., Wang, T., Wang, X.P., Xue, Q.W., Liu, L.C., 2008. Distribution and seasonal dynamics of roots in a revegetated stand of *Artemisia ordosica* Kracsh. in the Tengger Desert (North China). Arid Land Res. Manag. 22, 195–211.

Zhang, Z.S., Li, X.R., Liu, L.C., Jia, R.L., Zhang, J.G., Wang, T., 2009. Distribution, bio-mass, and dynamics of roots in a revegetated stand of *Caragana korshinskii* in the Tengger Desert, northwestern China. J. Plant Res. 122, 109–119.

Zhou, X.Q., Chen, C.R., Wang, Y.F., Xu, Z.H., Hu, Z.Y., Cui, X.Y., Hao, Y.B., 2012. Effects of warming and increased precipitation on soil carbon mineralization in an Inner Mongolian grassland after 6 years of treatments. Biol. Fertil. Soils 48, 859–866.